Dynamic Ionization of Water under Extreme Conditions

Alexander F. Goncharov, Nir Goldman, Laurence E. Fried, Jonathan C. Crowhurst, I-Feng W. Kuo, Christopher J. Mundy, and Joseph M. Zaug

Lawrence Livermore National Laboratory, University of California, 7000 East Avenue, Livermore, California 94551, USA

(Received 21 July 2004; revised manuscript received 29 December 2004; published 1 April 2005)

Raman spectroscopy in a laser heated diamond anvil cell and first principles molecular dynamics simulations have been used to study water in the temperature range 300 to 1500 K and at pressures to 56 GPa. We find a substantial decrease in the intensity of the O-H stretch mode in the liquid phase with pressure, and a change in slope of the melting line at 47 GPa and 1000 K. Consistent with these observations, theoretical calculations show that water beyond 50 GPa is ''dynamically ionized'' in that it consists of very short-lived (<10 fs) H_2O, H_3O^+, and OH^- species, and also that the mobility of the oxygen ions decreases abruptly with pressure, while hydrogen ions remain very mobile. We suggest that this regime corresponds to a superionic state.

DOI: 10.1103/PhysRevLett.94.125508 PACS numbers: 62.50.+p, 61.20.Ja, 64.70.Ja, 78.30.Cp

The behavior of water at conditions of extreme pressure and temperature is of profound importance to planetary science, geoscience, and fundamental chemistry. Of particular interest is the conductivity of water. It is this conductivity, for example, that may account to a large extent for the observed magnetic fields of Neptune and Uranus [1]. To date there has been no experimental indication of conductivity in the solid state. A superionic phase has been theoretically predicted above 20 GPa and at 2000 K [2]. In this case the oxygen atoms form a lattice that is isostructural to crystalline ice VII, while the protons hop between different molecular sites [2]. The predicted superionic phase of H_2O is unusual in that it involves elements known to form strong covalent bonds under ambient conditions. It is thus a striking example of the ability of extreme pressure to disrupt covalent interactions. Contrary to the predictions of Ref. [2], calculations performed more recently [3,4] show large oxygen diffusion at twofold compression (corresponding to a pressure of about 22 GPa), characteristic of a fluid state.

Until recently, the experimental study of water at extreme conditions was limited mainly to shock–wave compression investigations [5,6]. Electrical conductivity shows a rapid increase up to 30 GPa, but only a weak dependence at higher pressures. This plateau of conductivity has been attributed to the complete chemical ionization of the water molecule. However, the results of a Raman study of shock-compressed water [6] show the persistence of H_2O molecules and the near absence of hydrogen bonding (dominant at 12 GPa) at 26 GPa. Static diamond anvil cell (DAC) experiments have been mostly limited to the solid phase below the melting curve (ice VII above 2 GPa) and also the melting curve itself [7–11]. Raman measurements of liquid water under static high-pressure conditions have up to now been limited to 22 GPa [12,13].

In this Letter we report Raman spectra of ice and liquid water obtained *in situ* using a laser heated DAC over a wide range of pressure (5 to 56 GPa) and temperature (300 to 1500 K) combined with molecular dynamics (MD) simulations under similar conditions (11–122 GPa and 1000–2000 K). High-temperature Raman data allowed us to construct the phase diagram while theoretical calculations have been performed to obtain a deeper insight into the dynamics of the molecular dissociation and ionization. Our most important observation is that there is a sudden change in the slope of the melting curve at 47 GPa and 1000 K. Moreover, the Raman spectra of a translational mode of ice change in the vicinity of this triple point, where a liquid and two solid phases meet. We also find that the O-H stretch mode in the liquid gradually decreases in intensity and is barely observable above 50 GPa. In agreement with these observations, first principles simulations show an apparent transition to a superionic state above 47 GPa, higher than previous predictions [2]. The MD simulations show that water at ca. 40–70 GPa and 1000–2000 K consists of very short-lived H_2O, H_3O^+, and OH^- species (<10 fs).

We performed the experiments using a DAC with diamonds having flats of between 200 and 500 μm diameter depending on the required pressure. A rhenium gasket was used to contain the sample. A continuous-wave 50 W Nd:YAG (Nd-doped yttrium aluminum garnet) laser was used as the heating source. To provide efficient heat transfer to the sample we placed in the gasket cavity a $50 \times 50 \times 10$ μm plate of a Pt-Ir (20% Ir) alloy with a central hole of diameter of approximately 10 μm. This hole formed a sample cavity that ensured radially symmetric heating and allowed us to probe the whole sample in the axial direction to increase the signal. In some of the lower-pressure experiments (to 25 GPa), in order to further reduce thermal gradients, the sample was thermally insulated from the diamond anvils by smooth alumina plates of approximately 5 μm thickness. Similar spectra were found with and without the use of alumina plates. Experimental scans were performed quasi-isobarically in the pressure range from 5 to 56 GPa and from temperatures of 700 to 1600 K. The sample was first compressed at room temperature and subsequently heated. As described below the experimental temperature range was sufficient to melt the

sample. Raman spectra did not show any sign of chemical reaction with the solids in the DAC (there was no sign of, for example, low-frequency Raman modes that may be associated with a metal oxide). Experiments were also performed rapidly to reduce the possibility of chemical reaction. The data collection time was roughly 5 s, with 20 s between successive temperatures. We always verified that the Raman spectra at ambient temperature were unchanged after the experiment. Furthermore, the water sample was transparent and uncolored before and after the experiment.

Our confocal Raman system has previously been described in detail [14]. We used the 458 nm line of a 300 mW Ar ion laser to excite the Raman spectra. A Mitutoyo near IR 20× long-working distance objective lens was employed for the collection of Raman spectra in the backscattering geometry. The Raman spectra were collected in the relative wave number range of -4000 to 4000 cm^{-1} in one spectral window. The YAG laser radiation was introduced into the Raman system using polarizing beam-splitter cubes and was focused to a 20–30 μm spot using the same objective lens. Controlled attenuation of the YAG beam was achieved using a combination of a polarizing beam-splitter cube and $\lambda/2$ wave plate.

We attempted to determine the temperature of the sample by fitting the Planck function to the thermal radiation emitted by the metal plate. We also estimated temperature by analyzing the relative intensities of the Stokes and anti-Stokes peaks. We found that this method yields substantially lower temperatures compared to the radiometric method if the hole in the plate was probed. Consistent results were obtained if the Raman spectra were collected from a point on the surface of the plate rather than from the hole. We adopted the Stokes-to–anti-Stokes intensity technique because it is based on an intrinsic property of the studied system and, moreover, because it gives results that are more consistent with other observations (see below). Pressure was determined at room temperature using a conventional ruby manometer before and after laser heating (which was the same within the experimental error in most cases). Thermal pressure due to laser heating was estimated not to exceed 1 GPa and was neglected for simplicity [15].

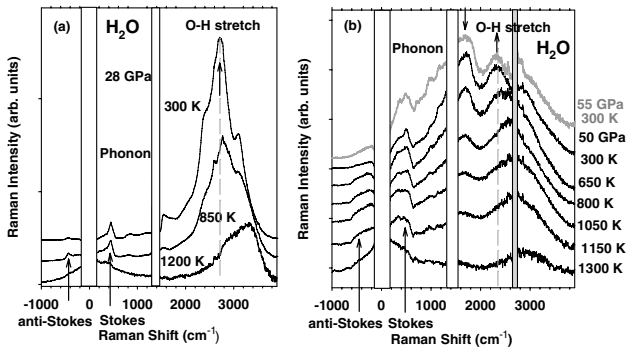

FIG. 1. The temperature dependence of Raman spectra of H_2O at 28 GPa (a) and 50 GPa (b). The spectrum at 55 GPa and 300 K (gray curve) is also shown in (b) for comparison. Pressure was measured at room temperature. The Raman spectra are normalized using a white light source of known spectral distribution. The Raman signal corresponding to the second-order scattering from the diamond anvils is subtracted [16]. The shaded area masks a numerical artifact (substantial only at high pressures) due to this procedure in the vicinity of the diamond second-order peak. The rectangles centered at zero frequency and near 1332 cm^{-1} mask differential peculiarities associated with the subtraction of elastically scattered radiation and the diamond first-order peak. The dashed vertical lines correspond to the position of the O-H stretch band in ice VII.

The Raman spectra of the ice VII solid phase show a drastic change upon heating in the region of the O-H stretch (Fig. 1). In the ice VII phase under pressure the frequencies of this O-H multiplet soften and couple to other excitations [e.g., at 1650 cm^{-1}, Fig. 1(b)], which may be ascribed to a strengthening of the hydrogen bond [16–18]. The frequencies of all components of the O-H band increase with temperature (Fig. 1) indicating that the hydrogen bond in ice VII weakens as the melting transition is approached and molecules acquire larger translational disorder. To determine the melting of ice VII, we monitored the behavior of the translational (phonon) mode. This band broadens significantly and changes shape (additional intensity appears at lower frequencies as the result of a breakdown of the wave-vector conservation rule) when melting occurs, while in the solid phase the corresponding degree of temperature-induced broadening is very moderate. Also, rotational modes (near 800 cm^{-1} at 28 GPa) disappear upon melting. Concomitantly, changes also occur in the O-H band: a broad doublet is observed in the liquid that has a different intensity distribution compared to that in ice VII (see also Ref. [13]). The phonon mode of ice VII broadens substantially at 53 GPa and 300 K [Fig. 1(b); see also Ref. [16]] due to transformation to a dynamically disordered ice VII phase [19]. A similar change occurs when heating ice VII at 50 GPa [Fig. 1(b)], which allowed us to trace the corresponding transformation line (see below). All the changes in Raman spectra observed on heating are reversible.

First principles Car-Parinello [20] density functional MD simulations of liquid water were conducted at 1000, 1200, 1500, and 2000 K at densities of 1.49–3.0 g/cc (11–122 GPa). We used CPMD v.3.91 [20], with the Becke-Lee-Yang-Parr exchange correlation functional [21], Troullier-Martins pseudopotentials [22] for both oxygen and hydrogen, and a system size of 54 H_2O molecules. A plane wave cutoff of 120 Ry was used in all simulations in order to ensure convergence of the stress tensor. After equilibration with velocity scaling, the temperature was controlled with Nose-Hoover thermostats [23] for all nuclear degrees of freedom. A value of 200 a.u. was chosen for the fictitious electron mass. The simulation time step was 0.048 fs (ca. 2 a.u.). Simulations were performed with steps of 0.1–0.2 g/cc between neighboring densities. Equilibration runs were performed for 2 ps at each density studied,

starting from a configuration at a lower density. Data collection runs were performed for 5–10 ps.

Determination of the oxygen diffusion constants at 1000–2000 K shows freezing into a glasslike state with mobile protons (Fig. 2), in qualitative agreement with the superionic phase predicted in Ref. [2]. The glass transition, however, is found at substantially higher pressures than reported in Ref. [2]. Simulations in which ice VII was heated at constant density gave a qualitatively similar (within 10 GPa) melting transition point. Molecular concentrations and lifetimes were analyzed on the basis of the O-H bond distance. The O-H bond distance cutoff was determined to be the position of the maximum in the O-H potential of mean force at the simulated density and temperature. At 1200 K and 2.0 g/cc (30 GPa) we observe that H_2O is the dominant species, with the presence of short-lived H_3O^+ and OH^- (not shown). This observation is consistent with simulations at nearly the same conditions of Schwegler *et al.* [4]. By 2.31 g/cc, the point at which the oxygens freeze, we observe H_2O lifetimes that are less than one O-H bond vibration period, i.e., 10 fs, and as such are too short lived to be labeled as molecules, *per se*. We term this a ''dynamically ionized'' state.

Under increasing pressure the Raman spectra of liquid water decrease in intensity in the spectral range of the O-H stretch vibration [Fig. 3(a)]. The theoretically computed power spectra [Fig. 3(b)] show qualitatively similar behavior. The observed pressure changes are in good agreement with the results of lower-pressure static experiments [12,13]. Our spectra are also qualitatively similar to those observed in shock compression experiments [6].

The observed change of intensity of the O-H stretch in the Raman spectra of liquid water with pressure implies alteration of the local atomic structure and the bonding properties. At lower pressure (below approximately 12 GPa) liquid water has a predominantly molecular character. The Raman spectra reveal only moderate changes with pressure in this regime [12]. At higher pressure our data show a decrease in intensity and a broadening of the O-H stretch. This is consistent with the theoretically predicted decrease of the lifetime of the H_2O molecule (Fig. 2).

Using Raman spectroscopy, we have mapped out the phase boundaries between ice VII, disordered ice VII, and the liquid phase (Fig. 4). We determined melting by observing characteristic Raman spectra corresponding to each state of matter (cf. Refs. [7,9,11]). Our data agree within the precision of our measurements with the results of Refs. [8,9,13]. The melting curve shown in Fig. 4 shows a change in slope above 47 GPa and 1000 K. Similar behavior was observed in Ref. [10] and interpreted as being due to the presence of the triple point between liquid water, ice VII, and ice X (albeit at substantially higher temperature). Based on experimental and theoretical results [16,19,24] and the results of this work we instead propose a dynamically disordered ice VII [19] (which becomes the superionic phase at higher temperature) as the high-pressure solid phase. We suggest that the difference between those two states is determined by the character of the mobility of the protons; protons are largely localized in the dynamically disordered ice VII but become highly mobile (thus contributing to charge transport) in the superionic phase. The observed phase line, corresponding to melting of the superionic phase, is in good agreement with the theoretically calculated line. Upon passing to the superi-

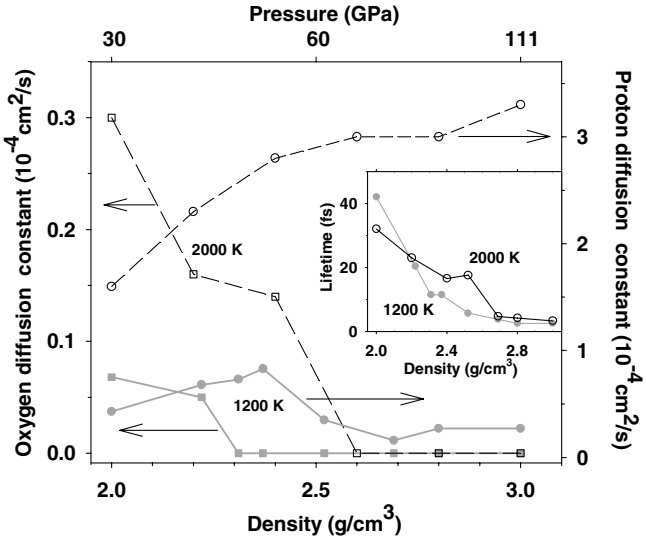

FIG. 2. Calculated diffusion constants for oxygen and protons at 1200 and 2000 K. Inset: the lifetime of an H_2O molecule as a function of density at 1200 and 2000 K. All other species lifetimes were found to be less than 5 fs for all densities investigated at this isotherm.

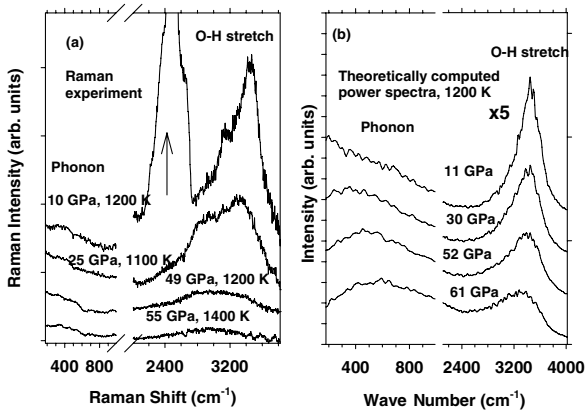

FIG. 3. Raman spectra of liquid water as a function of pressure: experimentally observed spectra (a) and theoretically computed power spectra at 1200 K (b). The Raman signal corresponding to the second-order scattering from the diamond anvils (indicated by the arrow in the 10 GPa spectrum) is subtracted for traces corresponding to pressures above 10 GPa. The Raman spectra are normalized (see the Fig. 1 caption). Note that the power spectra do not take into account any selection rules, so that observed intensity ratios should not necessarily be reproduced. To facilitate the comparison between theory and experiment, two panels of the theoretical spectra are shown on different intensity scales.

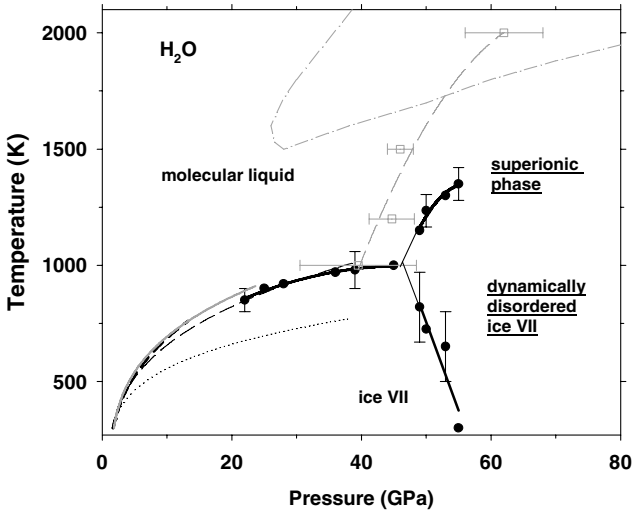

FIG. 4. Phase diagram of H_2O. Solid circles correspond to the transformation points determined from the spectral data. Corresponding temperatures were chosen to be midpoints between experimentally determined temperatures in the various phases (see the text). Thick solid lines are guides to the eye for our experimental results; thin solid lines are extrapolations of the measured lines. Gray squares and the dashed line (guide to the eye) correspond to theoretically computed conditions for the freezing of oxygen. Thick, thin black dashed, gray dotted, and gray solid lines are interpolated data from Refs. [8,9,11,13], respectively. Data from the Ref. [10] are much higher in temperature and are not shown. The gray dot-dashed line corresponds to the previously proposed [2] boundary of the superionic phase. The boundary between the dynamically disordered ice VII and superionic phase has not yet been determined.

onic phase, a much steeper slope in the melting line is observed. This may be attributed to the likely large change in entropy of the superionic state compared with ice VII and by consideration of the Clausius-Clapeyron condition ($dT_m/dP_m = \Delta V_m/\Delta S_m$).

In conclusion, our combined experimental and theoretical investigation of water under extreme conditions suggests a superionic phase above 47 GPa, a pressure roughly twice that predicted in Ref. [2]. This superionic phase consists of very short-lived (<10 fs) H_2O, H_3O^+, and OH^- species. Given that bound molecules are not present, we call superionic water dynamically ionized. The proposed dynamical mechanism of dissociation of hot, compressed water is important for a better understanding of chemistry under extreme conditions. This work also determines the phase diagram of water under conditions relevant to planetary science and geophysics. The measured and calculated phase line between the liquid and the superionic state is steeper than that reported in [2], which suggests that the Neptune isentrope intersects the solid superionic state. This contrasts with the predictions of [2], where only fluid phases of water were found along the planetary isentrope.

We thank the following individuals for many valuable discussions: R. J. Hemley, J.-F. Lin, V. Struzhkin, E. Gregoryanz, E. Schwegler, T. Ogitsu, C. S. Yoo, M. Nicol, and R. Boehler. We are grateful to D. Hansen for technical assistance. This work was performed under the auspices of the U.S. Department of Energy by the University of California, Lawrence Livermore National Laboratory under Contract No. W-7405-Eng-48.

[1] N. F. Ness *et al.*, Science **233**, 85 (1986); **246**, 1473 (1989).
[2] C. Cavazzoni *et al.*, Science **283**, 44 (1999).
[3] E. Schwegler, G. Galli, and F. Gygi, Phys. Rev. Lett. **84**, 2429 (2000).
[4] E. Schwegler, G. Galli, F. Gygi, and R. Q. Hood, Phys. Rev. Lett. **87**, 265501 (2001).
[5] A. C. Mitchell and W. J. Nellis, J. Chem. Phys. **76**, 6273 (1982); R. Chau, A. C. Mitchell, R. W. Minich, and W. J. Nellis, J. Chem. Phys. **114**, 1361 (2001).
[6] N. C. Holmes, W. J. Nellis, W. B. Graham, and G. E. Walrafen, Phys. Rev. Lett. **55**, 2433 (1985).
[7] Y. Fei, H.-K Mao, and R. J. Hemley, J. Chem. Phys. **99**, 5369 (1993).
[8] F. Datchi, P. Loubeyre, and R. LeToullec, Phys. Rev. B **61**, 6535 (2000).
[9] N. Dubrovinskaia and L. Dubrovinsky, High Press. Res. **23**, 307 (2003).
[10] B. Schwager, L. Chudinovskikh, A. Gavriliuk, and R. Boehler, J. Phys. Condens. Matter **16**, S1177 (2004).
[11] M. Frank, Y. Fei, and J. Hu, Geochim. Cosmochim. Acta **68**, 2781 (2004).
[12] T. Kawamoto, S. Ochiai, and H. Kagi, J. Chem. Phys. **120**, 5867 (2004).
[13] J.-F. Lin *et al.*, J. Chem. Phys. **121**, 8423 (2004).
[14] A. F. Goncharov *et al.*, in *Science and Technology of High Pressure*, edited by M. H. Manghnani, W. J. Nellis, and M. F. Nicol (Universities Press, Hyderabad, India, 2000), p. 95.
[15] A. Dewaele, G. Fiquet, and Ph. Gillet, Rev. Sci. Instrum. **69**, 2421 (1998).
[16] A. F. Goncharov, V. V. Struzhkin, H.-K. Mao, and R. J. Hemley, Phys. Rev. Lett. **83**, 1998 (1999).
[17] K. P. Hirsch and W. B. Holzapfel, J. Chem. Phys. **84**, 2771 (1986).
[18] G. E. Walrafen *et al.*, J. Chem. Phys. **77**, 2166 (1982).
[19] M. Benoit, A. H. Romero, and D. Marx, Phys. Rev. Lett. **89**, 145501 (2002).
[20] R. Car and M. Parrinello, Phys. Rev. Lett. **55**, 2471 (1985); CPMD, version 3.91, copyright IBM Corp., 1990–2004, copyright MPI fuer Festkoerperforschung Stuttgart, 1997–2001; www.cpmd.org.
[21] A. D. Becke, Phys. Rev. A **38**, 3098 (1988); C. Lee, W. Yang, and R. C. Parr, Phys. Rev. B **37**, 785 (1988).
[22] N. Troullier and J. L. Martins, Phys. Rev. B **43**, 1993 (1991).
[23] S. Nosé, Mol. Phys. **52**, No. 2, 255 (1984); W. G. Hoover, Phys. Rev. A **31**, 1695 (1985).
[24] A. Putrino and M. Parrinello, Phys. Rev. Lett. **88**, 176401 (2002).